Indian Journal of Advances in Chemical Science

Article

Ambient Ionization Mass Spectrometry in Biomedical Research: An Overview

Bharath Kumar*

Independent Researcher, Chennai - 600 061, Tamil Nadu, India

ABSTRACT

Analytical chemistry has undergone a revolution thanks to ambient ionization mass spectrometry (AIMS), which makes it possible to analyze samples quickly and directly in their natural state. The analytical community has led the continued development of AIMS since its inception almost 20 years ago, spurred on by the plethora of benefits it offers in addition to conventional mass spectrometry (MS). Since the development of desorption electrospray ionization MS, ambient MS techniques have become more popular in a range of disciplines, including food science and health. Because it requires little sample preparation and offers quick, direct analysis of samples in a range of physical states, AIMS is gaining popularity in the domain of metabolomics. Consequently, attention in AIMS has rapidly grown among analytical communities around the world, and AIMS methodologies are becoming more and more ingrained in regular laboratory procedures. This annual review describes the use of AIMS in 2022 with an emphasis on biomedical applications. Even though some new methods are being developed, AIMS research is increasingly committed to improving the methods that already exist, particularly in terms of repeatability, quantification, and functionality.

Key words: Ambient ionization, Atmospheric ionization, Desorption ionization, Mass spectrometry imaging

1. INTRODUCTION

The atmospheric desorption and ionization of sample analytes in their natural setting are made possible by ambient ionization mass spectrometry (AIMS) techniques, and there are many benefits of AIMS over conventional benchtop techniques [1]. The removal of chromatographic technique enables sample assessment rapidly, the reduction or elimination of time-consuming extraction steps, and the applicability of ambient ionization sources for on-site when used in combination with portable instruments. As a result, a growing number of scientific disciplines is becoming aware of the potential applications of AIMS, particularly in the fields of forensics, homeland security, and environmental sciences, as well as disease diagnostics. The limitations of traditional bench top MS techniques have been a hindrance in all these fields, as well as many others, and could be significantly enhanced by rapid, on-site analysis. AIMS-based disease diagnostics has the capacity to significantly reduce wait times for test results with point-of-care testing; criminal investigations could be concluded more quickly by analyzing forensic evidence at the crime scene; and environmental sample analysis could be completed on-site without the time-consuming shipment of samples from distant locations.

As more and more research fields learn about the potential benefits of AIMS, every year brings new methods, advancements in tried-and-true techniques, and fascinating new applications. A summary of AIMS applications for 2022 will be given in this review. The sections that follow give a brief overview of AIMS techniques before going into detail about recent biomedical applications.

2. METHODOLOGY

This review focuses on research presented in peer-reviewed manuscripts published in recent years, with a specific focus on the most recent developments and biomedical applications of ambient ionization MS. The article must meet the following requirements to be considered for inclusion: (a) It must be published in a peer-reviewed journal; (b) it must be written in English; (c) the research must be empirical; and (d) it must address either an advancement or application of AIMS in the biomedical domain. To find peer-reviewed articles, Google Scholar was used as the electronic database. The following keywords were used: Ambient ionization, ambient MS drug monitoring, ambient MS drugs, ambient MS tumor, and ambient MS imaging. A total of 35 studies were included in the study.

The review is made up of three parts. The first section gives a summary of the different AIMS techniques. An overview of the AIMS techniques addressed through the review is listed in Table 1, along with information on their potential for use in the biomedical domain.

The second section gives an overview of the various scientific questions and real-world issues that have been addressed by AIMS methods in the biomedical field. The third section examines technological advancements in the domain of AIMS.

3. AMBIENT IONIZATIN TECHNIQUES

Desorption electrospray ionization (DESI) technique was the first ambient ionization MS method to be published in the literature in

***Corresponding author:**
Bharath Kumar,
E-mail: bskumar80@gmail.com

ISSN NO: 2320-0898 (p); 2320-0928 (e)
DOI: 10.22607/IJACS.2023.1103002

Received: 27th May 2023;
Revised: 20th June 2023;
Accepted: 21st June 2023

Table 1: Common AIMS techniques identified through the review.

Acronym	Desorption mechanism	Ionization mechanism	Sampling process	Nature of research	Sample Ref #
DESI	Liquid extraction	Electrospray	Charged droplet jet surface desorption	Drug distribution in tissues, colorectal adenoma, bladder cancer, glioma samples, brain tumor, adenocarcinoma	
IR-MALDESI	Laser ablation	Electrospray	Matrix-assisted laser desorption	Metabolic profiling in neurodegenerative disease, brain metabolites, rat liver tissue imaging	
REIMS	Thermal desorption	Chemical/thermal evaporation		Oral cancer	
AFADESI	Liquid extraction	Electrospray	Charged droplet jet surface desorption	Spatially resolved metabolomics (thyroid tumor), disease biomarkers, exogeneous drug metabolites, CNS drug targets, hepatotoxicity of amiodarone	
nano-DESI	Liquid extraction	Electrospray	Charged droplet jet surface desorption	Uterus and brain tissue imaging, protein assembly in tissues	
LAESI	Laser ablation	Electrospray	Laser beam ablation/ desorption	Technical advancement	
PSI	Liquid extraction	Electrospray	Extraction, transportation by electric field	Sebum analysis, amins in urine	
EESI	Liquid extraction	Electrospray	Extraction using a neutral liquid spray	Drug monitoring	

DESI: Desorption electrospray ionization

October 2004 [2]. Soon after, DART approach was developed [3]. To make it easier for them to be used in an array of domains, such as clinical evaluation, including molecular imaging in tissue sections, both methods' designs and analytical performance have been continuously improved [4,5]. According to their desorption method, AIMS techniques can be broadly divided into three classes: Liquid based extraction, plasma desorption (PD), and laser ablation (LD). Several reviews provide detailed descriptions of the ionization techniques [4-6].

Many widely used AIMS methods fall under the category of solid-liquid extraction methods, which entail the extraction or desorption of analytes from a sample surface followed by ionization, frequently using a charged spray like in electrospray ionization (ESI). Plasma-based ionization methods use ionization processes like those found in ambient pressure ionization to produce reactive ions through an electrical discharge to facilitate ionization. Laser-based methodologies use an ultraviolet or infrared beam to ablate and desorb analytes from a sample to speed up sample analysis.

Substrate spray, direct liquid extraction, and spray-based extraction are the three different types of liquid extraction AIMS techniques. Spray-based techniques use a plume of droplets created by a solvent spray to desorb ions from the specimen surface, which the mass spectrometer then evaluates. These methods include EESI, SESI, DESI, and EASI ionization. Being one of the earlier AIMS techniques developed, the DESI method is without a doubt one of the most recognized and cutting-edge techniques. With DESI, when a plume of ionized tiny droplets collides with the sample's surface, secondary particles containing desorbed and ionized species are produced [2]. Ions are drawn into the mass spectrometer for analysis with the DESI technique placed in tandem to the MS orifice. DESI has undergone an array of alterations over time. AFADESI, a technique that uses a high-flow air stream to supplement analyte extraction and make droplets with desorbed analytes can be transported farther with less difficulty, has also been used in several recent studies [2,7-9]. The localized liquid extraction of materials is made possible by nanospray DESI (nano-DESI), which uses two tiny capillaries to create a liquid micro-junction on the analyte surface and a nebulizing gas to create charged droplets [10]. Since their creation, DESI and nano-DESI have become two of the most popular MS imaging (MSI) techniques [11]. DESI employs voltage to create an electrospray [1] to retrieve and ionize species from the specimen surface, while EASI sonic spray mechanisms to produce ions instead of a voltage bias [12].

The most well-liked substrate spray technique is known as paper spray ionization – "PS", which entails implementing a liquid analyte to a triangular portion of paper, letting it dry, then spraying the paper with a solvent, voltage, and placing the paper into the mass spectrometer [13]. Allowing interfering species from complex matrixes, like salts, to stick to the paper while soluble species are released and investigated frequently increases the sensitivity and reproducibility of this method. As a result, PS has shown the most potential for the quantification of analytes in clinical specimens when compared to other ambient ionization methods [14].

The liquid junction that forms between the analyte surface and a conductive pipette tip during LESA facilitates species extraction [15]. The method allows for quick and automatic surface sampling and has proven to be especially promising for imaging biological tissues. Recently, the method underwent further development to become microLESA, which was created to condense the sampling area that traditional LESA targets [16]. The MasSpec Pen uses an extraction method for ambient sampling, which is somewhat comparable to LESA [17].

Another variation of AIMS is paper spray ionization mass spectrometry (PS-MS). A spot of dried sample (such as biofluid) is typically analyzed using PS-MS, which is clipped to a high-voltage power source in front of a mass spectrometer. Analytes are electro sprayed after a spray solvent has been dispensed over the sample

spot, and then the mass spectrometer detects them. Therefore, using this method in ambient conditions, it is possible to quickly sample clinical sample for mass spectrometric analysis [18]. Because the entire workflow involves quicker analysis time, these features may make PS-MS an ideal point-of-care device for disease prognosis and clinical research [19].

A metallic needle, as opposed to paper, is typically used for specimen loading in touch spray (TS) ionization mass spectrometry (MS), a minor alteration of PS-MS [20-22]. By simply contacting the sample, the analytes are instantly absorbed into the needle tip. Following the application of high voltage to the needle tip, the remaining steps of the process are very comparable to those of PS ionization. Because of its ease of use and speedy sampling, TSI-MS is remarkably alluring for its low invasiveness and high throughput capabilities in clinical analysis.

During EESI-MS, dual jets of aerosols are combined, one of which is produced by ESI (Jingjing *et al.*, 2017; Gu *et al.*, 2012) [20,23]. Using liquid-liquid extraction, the sample is nebulized to create aerosol species, which are then bombarded with electrospray (ES) droplets. Gaseous-charged analytes for MS detection are created by the ES process' subsequent droplet evolution.

The use of lasers to accelerate sample desorption is very enticing because they can be optically concentrated to enable high efficiency desorption at improved spatial resolution and pulse frequencies than what is feasible with solvent- and plasma-based desorption approaches. LD ESI "LAESI" ablates a sample's surface [24]. As a result, a stream of desorbed species is created, and these molecules are later ionized by charged solvent species created by electrospray. Although less frequently used, the main benefit of laser-based techniques is their capacity for highly focused sampling, which is especially useful for MS imaging applications, and their capacity to decouple the desorption and ionization processes. The spatial resolution of LAESI is based on the diameter of the laser beam, which is typically operated at 200 μm [25]. Although there is no need for sample pretreatment or matrix addition in LAESI, samples must have a high-water content to effectively incur the IR beam and excite the target [25,26].

Initially, MALDESI was designed as a technique that combined the steps of MALDI sample preparation and LD with an ESI source for ionization. Therefore, samples had to be co-crystallized with an organic matrix for laser absorption, and then laser ablated with a UV laser, followed by ionizing the plume with an orthogonal ESI beam in sequence [27]. MALDESI's improvements have primarily concentrated on technical advancements for imaging applications, particularly its spatial resolution [28,29]. Initially, a UV laser was employed in this ionization process, but more recently, the use of an infrared (IR) laser (IR-MALDESI) has evolved [24]. Previously, due primarily to restrictions on the IR laser spot size, the spatial resolution in IR-MALDESI was limited to 150 μm. Higher lateral resolution for tissue imaging applications was made possible using a multielement optical system, which allowed the laser focal point to be shrunk to a 50 μm spot size.

REIMS is an AIMS technique that differs from other ambient ionization techniques in some ways, it does not fall under the categories mentioned above. In REIMS, biological tissues are removed using an electrocautery knife like those used in clinical surgery. By vaporizing the sample, the knife creates a plume of gas-phase analyte ions that are drawn into the mass spectrometer. Although REIMS was initially developed for analysis that differentiated healthy tissues from cancerous tissues during surgery, it has since been applied to a wider range of sample analyses [30].

4. BIOMEDICAL APPLICATIONS OF AIMS

4.1. Disease diagnosis

Undoubtedly, one of the most popular uses of AIMS is for disease diagnostics. The early detection of illness and infection, which frequently depends on time-consuming laboratory analyses like blood tests and tissue biopsies, is a significant barrier to effective medical treatment. It comes as no surprise that a primary clinical application of AIMS research is in the field of cancer. The field of cancer diagnostics may undergo a paradigm shift with the discovery of cancer-related biomarkers and the subsequent development of methods for their quick detection. Cancer's poor treatment outcomes and prognosis are significantly impacted by its metabolic heterogeneity. As a result, research keeps concentrating on finding fresh biomarkers and metabolic weaknesses, both of which rely on knowledge of altered metabolism in cancer.

Rapid diagnostics that are based on disease-related changes in the human metabolome have been actively pursued ever since the development of AIMS. DESI techniques have been widely used in biomedical research among solid-liquid extraction techniques. Among the DESI based techniques identified through the study, DESI-MSI (n = 11) technique was predominant in cancer and disease based diagnostic research. MS imaging "MSI" allows for the concurrent imaging of the spatial variability of numerous different biomolecules throughout the tissue specimen.

DESI-MSI was initially developed to rapidly assess the tissue metabolism under atmospheric conditions by simultaneously categorizing hundreds of molecules without labeling them [31,32]. Because it offers open-air sampling, DESI-MSI can be used to image tissues, without prior preparation. DESI-MSI is typically performed on a tissue section (15 μm thick), which is bombarded with a stream of charged tiny droplets traveling at high speeds that are created by electro spraying a solvent at a high voltage and using N_2 as a nebulizer [33,34]. These droplets moisten the tissue surface with the droplet solvent, dissolving biomolecules (mostly lipids and metabolites) that are present in the tissue. This liquid film is splashed, resulting in the formation of secondary species with the analytes, which are later converted into gaseous ions for mass spectrometric detection. A thorough biochemical (lipids and metabolites) mapping of the tissue is possible thanks to the use of an impinging spray of charged microdroplets to image the tissue surface in the x and y directions. Ion signals in the pixel-to-pixel mass spectra can then be mapped as 2D images.

Adenocarcinomas, which develop from the epithelial cells of the colorectal mucosa, make up many colorectal tumors [35]. Several MS modalities have been employed to examine the plasma, serum, and tissues of CRC patients. One investigation found that the metabolism of triacyl glycerides (TAG) and amino acids was dysregulated in CRC [36,37]. In addition, Shen *et al.* discovered that CRC tissues have increased glutathione metabolism to combat rising oxidative stress [38]. Studies investigating the connection between the metabolome and microbiota in CRC have also been published [39,40]. Despite extensive research into the genetic and molecular causes of CRC, metabolomic analysis of CRC tissue may provide new opportunities to find biomarkers that are diagnostic, prognostic, and predictive. Characterizing cell phenotype and metabolic activity, including the pathways that start or support malignant transformation, are possible using MS-based techniques. Nicol *et al.* (2022) carried out a feasibility study on human CRC patient samples containing malignant and adjacent non-neoplastic tissue along with their accompanying simulated biopsies to evaluate metabolic alterations in CRC and their ability to correlate with histology annotations and known biomarkers using DESI-MSI [41]. Following DESI analysis and H&E staining,

the spatial location of detected m/z ratios is preserved, enabling "gold standard" histological validation of the same slide [41]. Regardless of the tumor subtype, human CRC tissue analytes were randomly chosen from patients undergoing surgery and used to partner fresh and frozen representative CRC samples and biopsy samples that included non-tumor regions. The phosphatidylethanolamine (PE) ions existed in both the benign mucosa and adenocarcinoma in high concentrations. The spatial distribution of two additional species, *m/z* 480.307 and *m/z* 750.540), which were more specialized for benign mucosa, was consistent with the histopathology description for that tissue type. It was not a surprise that some ions existed in both areas because colorectal cancer frequently starts in the mucosal epithelial cells. Intriguingly, the histopathology examination of the samples showed two distinct tumor regions that were either next to the benign mucosa or next to the smooth muscle or serosa [41]. The tumor regions of interest "ROI" divided into two distinct clusters, one of which joined the benign ROIs in a single cluster, while the tumor ROIs close to the muscle or serosa formed a separate cluster [41]. Using histopathology spectra that were acquired by DESI, it was possible to identify colorectal adenocarcinoma with a recognition rate of more than 95%. One of the most obvious increases in ion abundance correlating with the CRC to long-chain and extremely long-chain fatty acids when compared to adjacent tissue types. Multiple phospholipids were discovered to be elevated in LVI-negative samples when adenocarcinoma regions were stratified according to LVI status. This finding suggests that DESI may be useful for both prognostic and diagnostic purposes [41].

DEFFI's appropriateness for imaging biological tissue with MS was investigated [42]. DESI performance with and without the flow focusing setup are also contrasted. The radial electrospray stream, elevated intensity, more adjustable variables, and improved ease of handling provided by the sprayer's robustness are the main potential benefits of using the flow focusing mechanism on DESI [42]. The fundamental concept behind flow focusing is that surface tension can be overcome by shear forces created by a co-flowing gas on a liquid flow, which restricts droplet formation at the aperture and leads to the creation of a plume of species. Although DEFFI-MSI has been used to identify exogenous compounds like drugs, [43-45] flow focusing on tissue samples has not yet been studied. The data from the porcine liver section were used to generate the presentation of findings, and the DEFFI was streamlined for image analysis of biological specimens in this work [42]. The image quality has improved compared to image quality from the DESI technique because of the obviously increased signal strength. The DEFFI study demonstrates more image sharpness when comparing the 25 µm pixel to the 50 µm pixel image data, proving that the sampling is inadequate to account for the smaller pixels. Although DEFFI is more sensitive than DESI, tissue integrity was not compromised, because H&E staining was done on the same specimen after acquisition (Figure 1). Increased DEFFI sensitivity also made it possible to structurally and spatially visualize low-intensity metabolites, such as the neurotransmitters glutamine, glutamate, and gamma-aminobutyric acid (GABA), which were challenging to assess using DESI. The performance improvement provided by DEFFI offers hope, the technique can be applied to a variety of biological and clinical studies, including the investigation of the function of neurotransmitters and molecules that are difficult to map within tissue using existing technologies [42].

Biological systems' physiologic functions are established in large part by endogenous metabolites. Numerous metabolites are involved in the pathophysiology of illnesses with high levels of interconnectivity [46,47]. By contrasting conventional DESI-MSI with ammonia assisted negative DESI/photoionization (aa-DESI/PI)-MSI, Pan et al. (2022) investigated metabolites in rodent brain tissue [48]. It was found that the combined effects of post-photoionization and ammonia additive substantially increased sensitivity of endogenous analytes when used in ambient conditions. In comparison to DESI, aa-DESI/PI can image 9 small metabolites (*m/z* 350) in rodent brain tissue and can produce signal intensities for metabolites that are up to 37.1-fold higher (Zhan *et al.*, 2023) [48].

The most typical form of cancer of the oral cavity is oral squamous cell carcinoma "OSCC." Electrocautery is a commonly used surgical technique for resecting the oral cavity because of its hemostatic function, which is necessary to cauterize the highly vascularized tissues. Radical resection of oral cavity cancer is still challenging. Rapid evaporative ionization MS "REIMS" has demonstrated great promise for intraoperative tumor and healthy tissue recognition [49]. Due to OSCC's infiltrative pattern of invasion, REIMS has trouble detecting limited numbers of tumor cells. The REIMS sensitivity was assessed by Seigel *et al.* (2022) to ascertain the minimum number of tumor cells that could be detected during oral cavity cancer surgery [50]. Eleven OSCC patients in total were included in the study. The tissue categorization based on 5 patients consolidated 185 REIMS metabolic profiles was contrasted to histopathology data using multivariate analysis. REIMS conducted four glossectomies while analyzing vapors *in vivo*. To support the REIMS findings, DESI-MSI was used to map tissue variability in 6 oral cavity sections. Using a novel cell-based assay made up of different cell lines (keratinocytes, myoblasts, and tumors), the sensitivity of REIMS was evaluated. With 96.8% accuracy, REIMS analysis distinguished between tumors and soft tissues. REIMS produced strong mass spectrometric signals *in vivo*. 90% of myoblasts and 10% of cancerous cells were detected by REIMS with 82.5% sensitivity and 81.5% specificity. The PE (O-16:1/18:2)/cholesterol sulfate metabolic shift that is shared by OSCC differentiation and mucosal maturation was highlighted by DESI-MSI [50].

The complexity of the proteome is dramatically increased protein post-translational modification "PTM," a process that goes far beyond what can be predicted based on the known protein-coding genes [51,52]. PTMs have a significant impact on the physiology of cells by altering the structure, interactions, transport, and function of proteins [53]. Proteoform identification, quantification, and spatial mapping are therefore essential for comprehending biological processes. The mapping of proteoform distribution in tissues remains difficult, even though top-down proteomics is a well-established field. The nano-DESI and AIMS techniques have been widely used for imaging lipids and metabolites with high sensitivity and a spatial resolution as low as 10 µm [54]. Only a few studies have used nano-DESI for protein imaging, even though its usefulness for protein analysis has been established [55]. Nano-DESI MSI has been employed to image protein complexes in rodent renal tissues, imaging in skin cancer, and protein distribution in regular and MYC-induced tumors in mouse brain tissue segments [56]. Laskin *et al.* (2022) used proteoform-selective nano nano-DESI MSI to image biological tissues [57]. The protein ions generated by nano-DESI directly on the tissue can be directly characterized with tandem MS. Proteoforms with distinctive PTMs were used to create ion images. 40 proteoforms (19 kDa) in total were discovered, of which 15 had confidence levels of 1, 9 had confidence levels of 2A, 1 had confidence levels of 3, and 10 had confidence levels of 4 (Smith *et al.*, 2019) [58]. The 14.1 kDa myelin basic protein and its various proteoforms were examined in relation to one another in the tissue. For a thorough understanding of the relevant biological pathways, the study offered the first insights into the variations in proteoform expression levels in various brain regions [57].

In this study, MBP and hemoglobin were the proteins with the highest concentrations of PTMs. Figure 2 shows pictures of six different MBP proteoforms. Mid and white matter regions of the brain demonstrated enhanced levels of both the N-terminally acetylated MBP (Figure 2a)

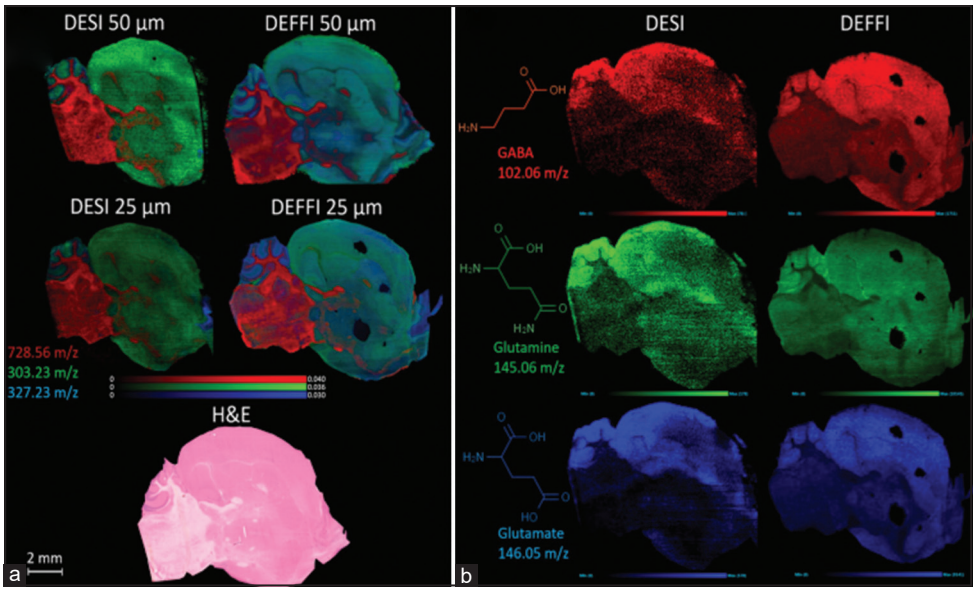

Figure 1: (a) Overlay ion images of PE(O-36:2) 728.56 m/z (red), fatty acid FA(22:6) 327.23 m/z (blue), and fatty acid FA(20:4) 303.23 m/z (green), with a pixel resolution of 50 µm (top) and 25 µm (bottom), compared between DESI (left) and DEFFI (right), on sagittal sections of a mouse brain, acquired in a negative ion mode. (b) Ion image for 3 low-intensity neurotransmitters in mouse brain: GABA 102.06 m/z (red), glutamine 145.06 m/z (green), and glutamate 146.05 m/z (blue), compared between DESI and DEFFI, on a mouse brain with a pixel resolution of 25 µm (Takats et al., 2022, ACS. Licensed under CC BY 2.0).

and its oxidized version (Figure 2b). Nevertheless, the midbrain region (Figure 2a) and the N-terminally oxidized MBP (Figure 2b) are where the N-terminally acetylated MBP is more prevalent (Laskin *et al.*, 2022). Due to the higher activity of MSR in the cerebellum region compared to other parts of the brain, the observed difference in the relative abundance of the two proteoforms may be explained. The phosphorylated MBP (Figure 2c) and its N-terminally acetylated form (Figure 2e) ratio images demonstrate a uniform distribution throughout the entire tissue section. On the other hand, the ratio image of the N-terminally acetylated, diphosphorylated MBP (Figure 2f) reveals the elevated abundance of this proteoform in the isocortex and hippocampal formation regions. The di-methylated and phosphorylated MBP was seen in an intriguing ratio image (Figure 2d), showing increased occurrence in the striatum ventral and thalamus zones. Using a combination of top-down proteomics and nano-DESI MSI on tissue specimen, the proteoform images of rat brain tissue have been generated. The individual proteoforms were conveyed differently in various tissue regions, as evidenced by ratio images [57].

Amyotrophic lateral sclerosis "ALS" is an idiopathic, life-threatening neurodegenerative disorder characterized by a gradual loss of motor function, with an average survival time of 2 to 5 years after diagnosis. A conclusive prognosis of ALS can be challenging owing to the absence of distinctive biomarkers and the heterogeneous disease phenotypes. Finding distinctive features to speed up the diagnosis process and increase diagnostic precision will require a thorough assessment of this disease. The diagnosis of ALS heavily relies on clinical procedures based on symptom presentation and progression, unlike other neurodegenerative diseases where clinical protocols are supplemented with medical testing [59-61]. Strong biomarkers and a deeper understanding of ALS's metabolic signature are urgently needed for accurate diagnosis and monitoring [62-64]. Proteomics-focused MS research has made significant contributions to the understanding of ALS and has revealed novel protein biomarkers that may be indicative of disease progression [65,66]. The analysis of metabolites in biological samples using MSI is appealing because it can measure the spatial and abundance distributions of analytes without the need for labeling [67-70]. The ambient ionization source IR-MALDESI MSI has unique benefits such as soft ionization and high salt tolerance [70-72]. An energy-absorbing ice layer is applied to the specimen in IR-MALDESI analyses prior to evaluation. The mid-IR laser then resonantly excites the water's O-H stretching bands to desorb neutral species, which are then electro spray ionized [72]. The matrix is advantageous because it makes it easier for analytes to desorb and ionize without adding extra molecule interference [73,74].

To compare post-mortem frontal cortex human brain tissues from patients with sporadic ALS "sALS" and those who had C9Pos, Muddiman *et al.* (2022) studied untargeted metabolomics by MSI [75]. The spatial variability and relative proportions of metabolites were evaluated for correlations with biological pathways using IR-MALDESI-MSI. As was already mentioned, IR-MALDESI's ability to detect metabolites was confirmed, and the ion images were placed correctly with pink colored blocks isolating the cohorts. Umoh *et al.*'s data were used to look for proteins that were involved in metabolite conversions. These proteins are identified with purple and white-filled circles denoting the presence or absence of the protein, respectively [75,76]. The study found glutamate to be dysregulated, which was particularly intriguing given how frequently glutamate is mentioned in ALS literature. Glutamate has been identified in an array of biological specimens, but its up- or down-regulation in relation to ALS has not been consistently reported [63,75]. The information that is currently available indicates that glutamate induces toxicity in neurons and oxidative stress in mitochondria, both of which promote neuronal apoptosis that may be connected to ALS [77-79]. This neurotransmitter is involved in crosstalk between various pathways and was discovered by IR-MALDESI. The study depicts the pathway for amino acid (glutamate, aspartate, and alanine) metabolism, which was reported in other studies and may have implications for the pathophysiology of ALS [63,77,80] and GABA, for instance, differ in their spatial distribution in that asparagine is only weakly detected in all patient samples while GABA is biased to specific tissue regions. Despite the fact that there is glutamate disorder between the control and C9Pos categories, this data do not clearly show any trends in metabolite

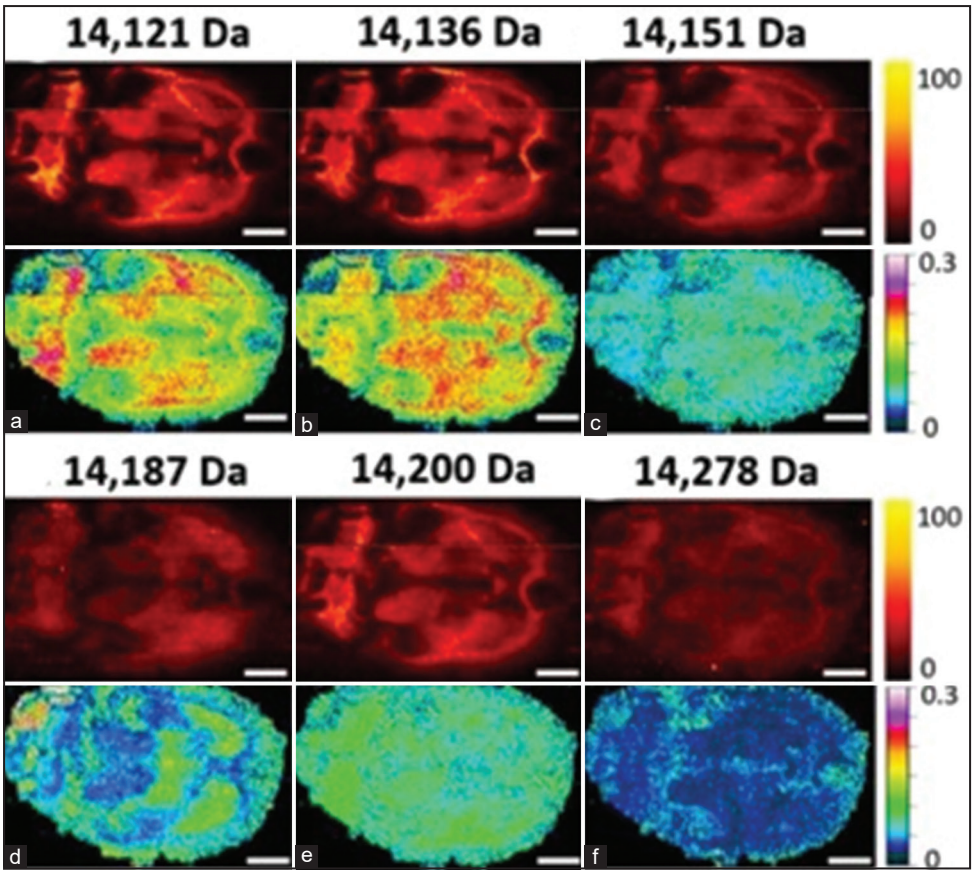

Figure 2: Ion images of the +19 charge state of the 14.1 kDa MBP proteoforms. Top panels show ion images normalized to the TIC. Bottom panels show images generated by plotting the ratio of the individual proteoform signal to the sum of signals of all the MBP proteoforms: (a) m/z 744.233519+, 14 121 Da, N-terminal acetylation (level 1), (b) m/z 745.023519+, 14136 Da, N-terminal acetylation, methionine sulfoxide (level 1), (c) m/z 745.813219+, 14151 Da, phosphorylation (level 3), (d) m/z 747.706319+, 14 187 Da, di-methylation, phosphorylation (level 2A), (e) m/z 748.390119+, 14200 Da, N-terminal acetylation, phosphorylation (level 2A), (f) m/z 752.492319+, 14 278 Da, N-terminal acetylation, di-phosphorylation (level 2A). Scale bar: 3 mm. Reproduced with permission from (Laskin *et al.*, 2022) by Angewandte Chemie.

regulation between disease cohorts [75]. However, this discovery is in line with proteomic findings in the literature [76].

4.2. Drug monitoring and metabolism

The failure rate for drugs intended to treat neurological disorders is very high [81,82]. Successful drug development for the central nervous system "CNS" depends on the deconvolution of potential targets. First off, choosing the wrong targets before a clinical trial is one of the critical reasons for high dropout rates [83]. In this regard, a deeper comprehension of binding targets may be helpful. Determining potential off targets can be just as important as figuring out how well CNS drugs work [84]. In addition, multi-targeted medications can be created for brand-new indications [85] or help with the creation of superior next-generation compounds [86].

The complex structure and operation of the brain make it particularly difficult to deconvolute CNS drugs for multiple targets. For better comprehension of how CNS drugs work, molecular neuroimaging, which offers *in vivo* and spatially resolved measures of neurobiology, has been effective [87]. Label-free MS imaging (MSI), which allows for simultaneous mapping of neurotransmitters, metabolites, and drugs in the brain [88-91] and is particularly helpful for probing brain metabolic heterogeneity, [88,89,92-94] has recently emerged as a promising molecular imaging tool.

A multi-target deconvolution approach for CNS drugs using AFADESI-MSI was investigated by Abliz *et al.* (2022) [95]. This approach couple's spatiotemporal metabolomics with isotope imaging. Drug-related differential metabolites were found using a spatially resolved approach and spatiotemporal analysis, and altered metabolic pathways, nodes, and positions were found after drug intervention using brain metabolic network matching and spatiotemporally resolved isotope tracing. The technique was applied to identify potential protein targets for the anti-insomnia drug candidate YZG-331 and offered a workable method of connecting metabolic biomarkers to protein targets in metabolic pathways [95]. It was discovered that the sedative- drug YZG-331 mainly accumulated in the pineal gland and only slightly entered the brain parenchyma. According to the findings, YZG-331 agonized LAT1 and OCT3 to export extracellular histamine in the periphery while also increasing GAD activity to produce more GABA in the hypothalamus. The suggested approach can offer visualization tools, new viewpoints on the efficacy and safety of CNS drugs, and assistance in understanding their mechanisms of action [95].

According to Iruzubieta *et al.* (2015), drug-induced liver injury "DILI" is a significant issue for drug development worldwide and a significant public health concern. Acetaminophen (APAP) overdose results in DILI in the developed world [96]. Because glucuronidation and sulfation reactions in the liver effectively metabolize APAP to form the nonoxidative metabolites APAP-glucuronide (APAP-GLUC) and APAP-sulfate (APAP-SULF), the drug is safe at therapeutic doses. Meanwhile, a minor component of APAP can form N-acetyl-

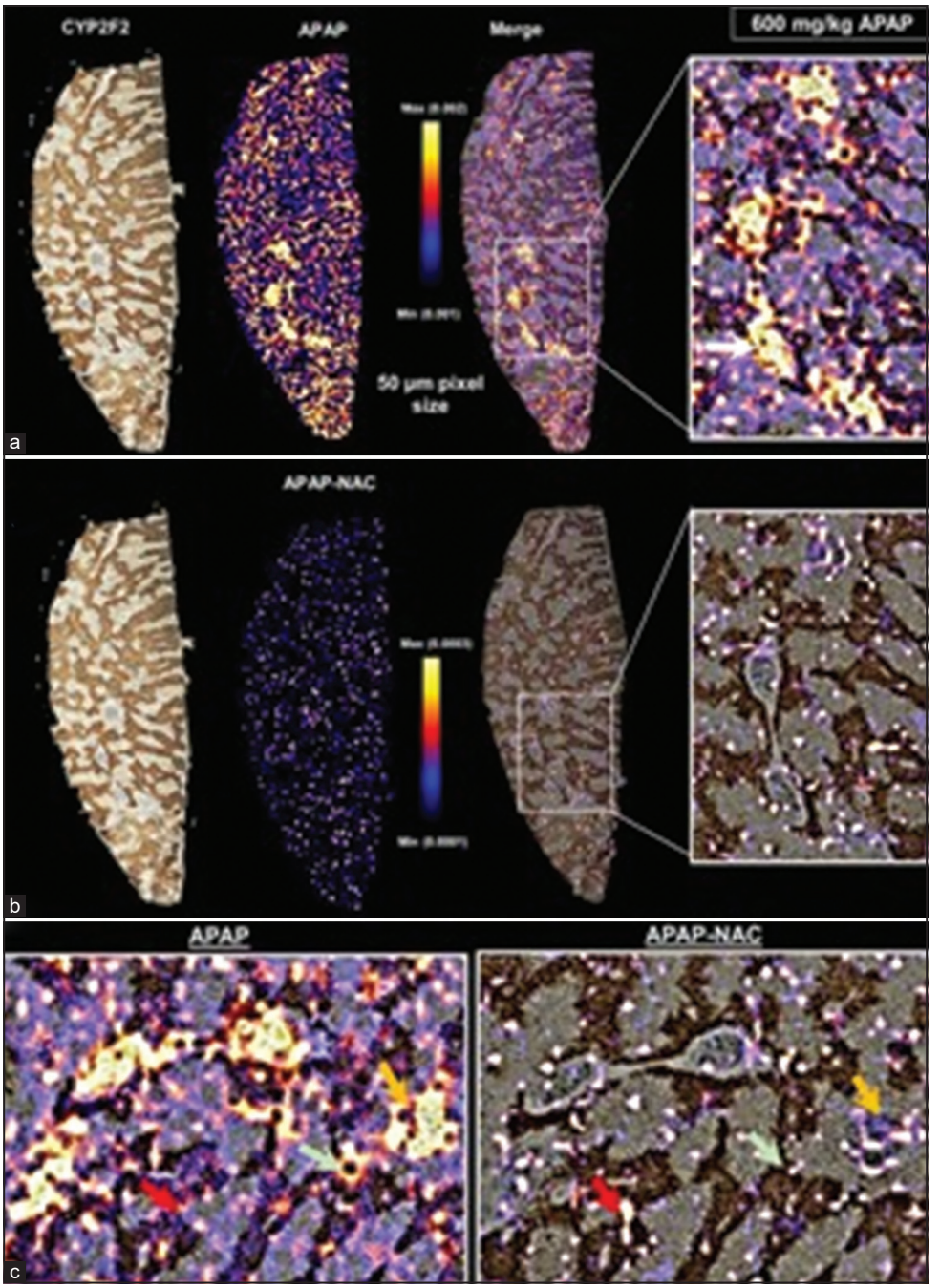

Figure 3: DESI-MSI analysis for spatial localization of APAP and APAP-NAC in liver sections at 50 µm pixel resolution after severe (600 mg/kg) APAP overdose: Fasted male C57BL/6J mice received 600 mg/kg APAP followed by sacrifice 30 min later. A representative photomicrograph of the cryo-section used for DESI-MSI and then immunostained for CYP2F2 is shown on the left. DESI ion images for APAP (a) and APAP-NAC (b) were then superimposed on the same liver cryo-section immunostained for CYP2F2 to generate merged images enlarged in panels on the right and expanded with rotation below (c). Reproduced with permission from (Ramachandran et al., 2022) by ACS.

p-benzoquinone imine, which is rapidly scavenged by hepatic glutathione stores [97,98]. to form the oxidative metabolites APAP-glutathione (APAP-GSH), APAP-cysteine (APAP-CYS), and APAP-N-acetylcysteine (APAP-NAC), preventing liver injury. However, after an excessive dose of APAP, the protective effect of GSH is overpowered by the increased NAPQI production, which starts an acute liver injury and ultimately results in centrilobular hepatocyte cell death.

LC-MS has typically been used to identify drug metabolism biomarkers in biofluids such as plasma, urine, or whole tissue homogenates, as in studies looking at acetaminophen metabolism [99-101]. Even though this analysis sheds some light on the prevalence of drugs or their metabolites, it does not provide data on regional concentrations of drug-derived metabolites that might be toxic to areas within individual organs or on local variations in drug metabolism within tissues. Radiolabels or antibodies have historically been used in traditional approaches to shed light on the spatial distribution of drugs [102,103]. Secondary metabolites, however, which can build up in the tissue and have toxic side effects, are often missed by these methods [104-107]. Using DESI-MSI analysis, Ramachandran *et al.* (2022) reported the spatial

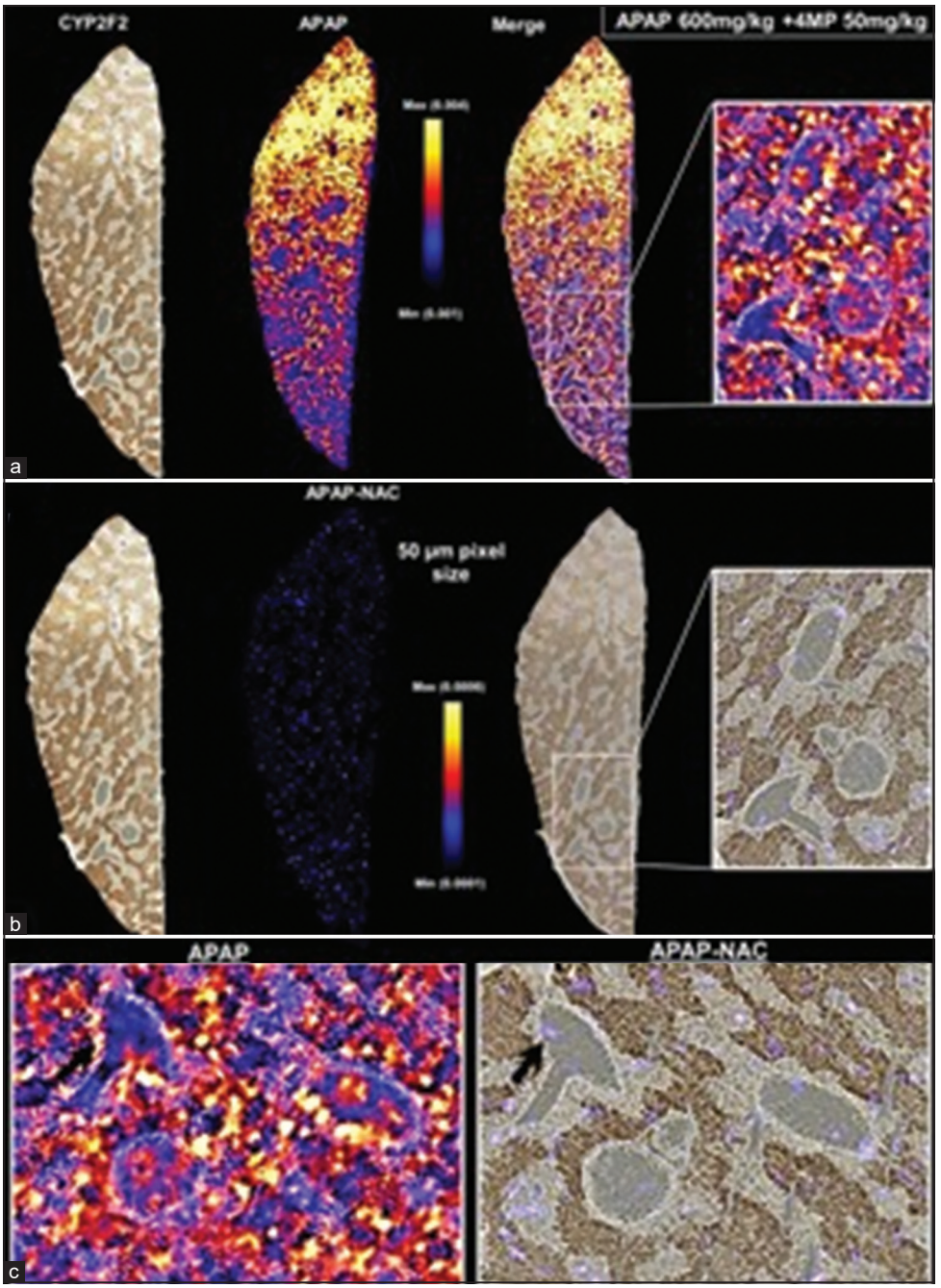

Figure 4: Effect of 4 MP on biodistribution of APAP and APAP-NAC captured with DESI-MSI analysis of liver tissue sections at 50 µm pixel resolution after severe (600 mg/kg) APAP overdose. Fasted male C57BL/6J mice received 600 mg/kg APAP followed by sacrifice 30 min later. A representative photomicrograph of the cryo-section used for DESI-MSI and then immunostained for CYP2F2 is shown on left. DESI ion images of APAP (a) and APAP-NAC (b) were then overlaid onto the same liver immunostained for CYP2F2 to generate merged images enlarged in panels on the right and expanded with rotation below (c). Reproduced with permission from (Ramachandran et al., 2022) by ACS.

visualization (Figure 3) of APAP metabolism within the liver following APAP overdose in the human-relevant C57BL/6J mouse model and showed alterations brought on by treatment with 4-methylpyrazole (4 MP) (Figure 4). To identify the locational concentration and propagation of oxidative and nonoxidative metabolites, mouse liver sections were examined following a variety of APAP overdoses [108]. In tissues, it was possible to detect distinct differences in signal intensities related to metabolite abundance, and 4 MP treatment significantly changed this topographical distribution. To characterize the spatial changes in APAP metabolite abundance following 4 MP treatment, the study provided a novel label- and matrix-free platform with high sensitivity. This cutting-edge imaging technology could be applied to further drug development for the prevention of APAP hepatotoxicity as well as research the effects of novel therapeutic interventions on molecular targets [108].

All facets of actions, including speech, reasoning, cognition, motion, and emotions, are controlled by the brain [109]. In addition, it has the most complex structure and operation. The functional variations in metabolic enzymes and blood circulation in brain sections affect drug efficacy and spatial distribution [110]. It is very challenging to develop

CNS drugs and describe the molecular mechanisms would happen for a specific drug, because many CNS drugs only have an effect after entering the brain. Understanding the drug's pharmacokinetics and pharmacodynamics are critical for drug development [111]. Creating novel technologies may open new possibilities and encourage the development of novel pharmaceuticals [112,113]. To provide high-coverage molecular profiles and microregional distribution information, He *et al.* (2022) created a temporo-spatial pharmacometabolomics technique using a high-resolution MS and an AFADESI-MSI system [114]. An investigation on the temporally and spatially changing levels of the CNS medication olanzapine (OLZ), as well metabolites in mouse brain over the duration and analysis of the drug's dynamics in the brain regions, served as the basis for the validation of this method [114].

Lipids are involved in a wide range of biological processes, including the movement of materials, the oxidation and reduction of energy, the recognition and transmission of information, cell development, differentiation, and apoptosis [115]. Glycerophospholipids assist in regulating the liver's lipid metabolism, fostering memory, boosting immunity, and delaying aging [116]. Brain cognitive function and lipid metabolism are related. Independent phospholipase A2 (iPLA2), which has been identified as a novel ferroptosis regulator by several studies, may play a role in the pathological progression of Parkinson's disease, which is primarily characterized by the inadequate repair of oxidized phospholipids [117,118]. The corpus callosum displayed the highest levels of phosphorylcholine and was markedly upregulated. The cerebral cortex displayed an up-regulation of glycerophosphocholine. The levels of PE were highly downregulated in the caudate putamen, and the cerebral medulla had the highest levels. In most microregions, glycerylphosphorylethanolamine showed upregulation. The pharmacokinetics of the hypnotic drug and its metabolites in various sections of the mouse brain were clearly demonstrated by this method. Furthermore, by mapping metabolic pathways, the pharmacodynamics of OLZ was demonstrated [114].

It is difficult to investigate how epimer drugs act *in vivo* and their varying metabolic profiles. MSI analysis can pictorially display the stereoscopic spread of compounds can provide a more thorough organ-specific profiling analysis. AFADESI-MSI was used by Abliz *et al.* (2022) in the development of a whole-body spatially resolved metabolomics. As illustrations, rats given varying oral doses of hypnotic drug candidates YZG-330 and YZG-331 [119]. Rich information that may help to explain why YZG-330's sedative-hypnotic effects are more notable than those of YZG-331 was discovered by comparing the differences in the relative concentrations of the drugs, their metabolic products, and neurotransmitters in rat whole-body tissue sections. It was interesting to note the elevated levels of GABA in the rats' brain and stomach. The study offered a practical and visual approach to investigate metabolic variations and shed light on the pharmacodynamic mechanisms underlying these prospective sedative-hypnotic drugs [119].

4.3. Technical advancement

Lipids are necessary parts of every cell and are crucial for many cellular processes. Lipids play several important roles in signal transduction, the regulation of vesicular protein transport, the recruitment of proteins to membranes, and the function of cell membranes as structural, thermal, and energetic components [120,121]. Because of their sophistication and structural diversity in biological samples, lipids are challenging to study at the molecular level. The most popular platform for both untargeted and targeted lipidomics studies is LC-MS [122,123]. The use of AIMS (Han *et al.*, 2005; Norris *et al.*, 2013; Xiao *et al.*, 2020; Wu *et al.*, 2013) [124,125] to directly image samples' molecular structures without sample pre-treatment is particularly relevant to this work. DESI [2] and nano-DESI [11] are examples of AIMS that have the unique ability to tailor the solvent composition to optimize analyte extraction from the sample [126,127], a critical first step in comprehending the function of MSI experiments in biological processes is to improve their lipid coverage. Although nano-DESI MSI can detect fatty acids and phospholipids, other lipid classes are hard to measure due to their relatively low concentration and poor ionization efficiency. Laskin *et al.* (2022) [128] investigated the impact of adding ammonium fluoride (NH4F) to the solvent. They measured the lipid enhancement factors when NH4F was present in the negative ionization mode. They found that using 500 M NH4F in 9:1 methanol: water enhanced lipid signals identified as [M-H] - ions by 10-fold to 460-fold. The effective proton abstraction from lipids is responsible for the observed signal augmentation. The interfacial pKa values of fatty acids are related with the enhancement factors that have been observed. The solvent composition allows for responsive imaging of both low and high abundance lipids without adversely affecting the noise level. Ammonium fluoride was found to significantly increase the sensitivity of MS imaging of lipids to the solvent [128].

Another widely used MSI technique DESI, which was developed from electrospray ionization and involves impacting the surface being studied with charged solvent droplets [2,5,129]. Due to the size of the electrospray sampling spot, the spatial resolution for DESI continues to be a problem [130]. In DESI-MSI, the spatial resolution is typically 150 m. The Vertes group has developed a new ambient electrospray-based MSI method called LA electrospray ionization MS (LA-ESIMS) to overcome this spatial constraint [131]. LA-ESI-MSI typically has a spatial resolution of about 100 m. Even though the spatial resolution can be increased using near-field optical techniques [132] or using a vacuum ultraviolet (VUV) [133] or extreme ultraviolet (EUV) [134] laser and transmission geometry optical systems [135-137]. It is challenging to combine ESI with these laser-sampling techniques to achieve high-spatial-resolution MSI under ambient conditions due to the complexity of these approaches. An enhanced high-spatial-resolution LA-ESI-MSI method utilizing a microlensed fiber was described by Zare *et al.* (2022) [138]. Only a few microns separated the sample surface from the fiber microlens in this experiment. This made it possible to sample craters that were close to the optical diffraction limit. The microlensed fiber (16 μm core diameter) used in this study was created by mechanical polishing and could produce a more precise laser focusing effect. The X-distance (from the sampling spot to the electrospray emitter in the horizontal direction) and Z-distance (from the sample surface to the mass spectrometer inlet in the vertical direction) were precisely optimized to achieve the highest signal intensity. To demonstrate imaging improvement with this high-resolution technique, the authors used the same slice of parsnip root tissue for both conventional LA-ESI-MSI and microlensed fiber desorption ESI-MSI [138].

Analyzing catecholamines (CAs) in biological matrixes is very interesting because these substances can be used as tumor-specific diagnostic markers [139-141]. Human endogenous substances known as CAs, such as dopamine (DA), epinephrine (E), and norepinephrine (NE), function as neurotransmitters and amine hormones [142] and influence bodily processes such as blood pressure, heart rate, and temperature regulation [143-146]. To detect or diagnose certain diseases, including neuroblastoma and pheochromocytoma, a tumor that develops from chromaffin cells of the adrenal medulla, the amount of CAs in urine is measured. About 15–20% of these tumors are extra-adrenal in origin and exhibit abnormal catecholamine secretion. Without the use of instrumental chromatography, Salentjin *et al.* (2022) created a boronate affinity paper spray MS method to increase selectivity and decrease ion suppression [147]. The boronate affinity

PS-MS clearly met the detection thresholds necessary to enable quick analysis of samples for clinical applications, such as the detection of pheochromocytomas (exceeding 0.5 g/mL) [147].

5. CONCLUSION

By making it possible to analyze samples quickly and directly in their natural state, AIMS has revolutionized the domain of analytical chemistry. With AIMS, workflows can be streamlined by doing away with sample preparation, analysis times can be drastically cut, and analysis outside of the traditional laboratory setting is now a real possibility. The most significant technological developments and novel AIMS applications in the biomedical sector for 2022 were highlighted in this review. Thanks to MS platforms that integrate numerous technologies and/or automate sampling, AIMS techniques are now more frequently used in clinical applications. The study also examined research that has been conducted to enhance the sensitivity and reliability of AIMS method analytical performance, allowing comparable performance to more conventional MS assays for specific applications like disease diagnosis and drug monitoring. The impact of AIMS will undoubtedly keep expanding as new methods are created and existing procedures are enhanced.

6. REFERENCES

1. D. J. Weston, (2010) Ambient ionization mass spectrometry: Current understanding of mechanistic theory; analytical performance and application areas, ***Analyst***, **135(4)**: 661-668.
2. Z. Takats, J. M. Wiseman, B. Gologan, R. G. Cooks, (2004) Mass spectrometry sampling under ambient conditions with desorption electrospray ionization, ***Science***, **306(5695)**: 471-473.
3. R. B. Cody, J. A. Laramée, H. D. Durst, (2005) Versatile new ion source for the analysis of materials in open air under ambient conditions, ***Analytical Chemistry***, **77(8)**: 2297-2302.
4. J. H. Gross, (2014) Direct analysis in real time--a critical review on DART-MS, ***Analytical and Bioanalytical Chemistry***, **406:** 63-80.
5. D. R. Ifa, C. Wu, Z. Ouyang, R. G. Cooks, (2010) Desorption electrospray ionization and other ambient ionization methods: current progress and preview, ***Analyst,*** **135(4)**: 669-681.
6. J. Laskin, I. Lanekoff, (2016) Ambient mass spectrometry imaging using direct liquid extraction techniques, ***Analytical Chemistry***, **88(1)**: 52-73.
7. Z. Luo, J. He, Y. Chen, J. He, T. Gong, F. Tang, ... & Z. Abliz, (2013) Air flow-assisted ionization imaging mass spectrometry method for easy whole-body molecular imaging under ambient conditions, ***Analytical Chemistry***, **85(5)**: 2977-2982.
8. Z. Luo, W. Wang, X. Pang, J. Zhang, C. Sun, X. Zhou, ... & Z. Abliz, (2021) Writing sequence identification of seals and signatures in documents using ambient mass spectrometry imaging with chemometric methods, ***Talanta***, **235:** 122804.
9. J. Zhang, X. Huo, C. Guo, X. Ma, H. Huang, J. He, ... & F. Tang, (2021) Rapid imaging of unsaturated lipids at an isomeric level achieved by controllable oxidation, ***Analytical Chemistry***, **93(4)**: 2114-2124.
10. M. Huo, Z. Wang, W. Fu, L. Tian, W. Li, Z. Zhou, ... & Z. Abliz, (2021) Spatially resolved metabolomics based on air-flow-assisted desorption electrospray ionization-mass spectrometry imaging reveals region-specific metabolic alterations in diabetic encephalopathy, ***Journal of Proteome Research***, **20(7)**: 3567-3579.
11. P. J. Roach, J. Laskin, A. Laskin, (2010) Nanospray desorption electrospray ionization: An ambient method for liquid-extraction surface sampling in mass spectrometry, ***Analyst***, **135(9)**: 2233-2236.
12. R. Haddad, R. Sparrapan, M. N. Eberlin, (2006) Desorption sonic spray ionization for (high) voltage-free ambient mass spectrometry, ***Rapid Commun Mass Spectrom***, **20(19)**: 2901-2905.
13. L. H. Li, H. Y. Hsieh, C. C. Hsu, (2017) Clinical application of ambient ionization mass spectrometry, ***Mass Spectrometry*** (***Tokyo***), **6(2)**: S0060.
14. H. Wang, J. Liu, R. G. Cooks, Z. Ouyang, (2010) Paper spray for direct analysis of complex mixtures using mass spectrometry, ***Angewandte Chemie***, **122(5)**: 889-892.
15. C. L. Feider, A. Krieger, R. J. DeHoog, L. S. Eberlin, (2019) Ambient ionization mass spectrometry: Recent developments and applications, ***Analytical Chemistry***, **91(7)**: 4266-4290.
16. V. Kertesz, G. J. Van Berkel, (2010) Fully automated liquid extraction-based surface sampling and ionization using a chip-based robotic nanoelectrospray platform, ***Journal of Mass Spectrometry***, **45(3)**: 252-260.
17. D. J. Ryan, N. H. Patterson, N. E. Putnam, A. D. Wilde, A. Weiss, W. J. Perry, ... & J. M. Spraggins, (2019) MicroLESA: Integrating autofluorescence microscopy, *in situ* micro-digestions, and liquid extraction surface analysis for high spatial resolution targeted proteomic studies, ***Analytical Chemistry***, **91(12)**: 7578-7585.
18. J. Zhang, J. Rector, J. Q. Lin, J. H. Young, M. Sans, N. Katta, ... & L. S. Eberlin, (2017) Nondestructive tissue analysis for *ex vivo* and *in vivo* cancer diagnosis using a handheld mass spectrometry system, ***Science Translational Medicine***, **9(406)**: eaan3968.
19. J. Liu, H. Wang, N. E. Manicke, J. M. Lin, R. G. Cooks, Z. Ouyang, (2010) Development, characterization, and application of paper spray ionization, ***Analytical Chemistry***, **82(6)**: 2463-2471.
20. L. Jingjing, H. Xiaowei, H. Yan, Y. Muqian, B. C. Le Jiang, (2017) Development and application of paper spray ionization mass spectrometry, ***Progress in Chemistry***, **29(6)**: 659.
21. K. S. Kerian, A. K. Jarmusch, R. G. Cooks, (2014) Touch spray mass spectrometry for *in situ* analysis of complex samples, ***Analyst***, **139(11)**: 2714-2720.
22. D. R. Ifa, L. S. Eberlin, (2016) Ambient ionization mass spectrometry for cancer diagnosis and surgical margin evaluation, ***Clinical Chemistry***, **62(1)**: 111-123.
23. H. Gu, N. Xu, H. Chen, (2012) Direct analysis of biological samples using extractive electrospray ionization mass spectrometry (EESI-MS), ***Analytical and Bioanalytical Chemistry***, **403:** 2145-2153.
24. P. Nemes, A. Vertes, (2007) Laser ablation electrospray ionization for atmospheric pressure, *in vivo*, and imaging mass spectrometry, ***Analytical Chemistry***, **79(21)**: 8098-8106.
25. P. Nemes, A. S. Woods, A. Vertes, (2010) Simultaneous imaging of small metabolites and lipids in rat brain tissues at atmospheric pressure by laser ablation electrospray ionization mass spectrometry, ***Analytical Chemistry***, **82(3)**: 982-988.
26. Y. P. Yung, R. Wickramasinghe, A. Vaikkinen, T. J. Kauppila, I. V. Veryovkin, L. Hanley, (2017) Solid sampling with a diode laser for portable ambient mass spectrometry, ***Analytical Chemistry***, **89(14)**: 7297-7301.
27. J. S. Sampson, A. M. Hawkridge, D. C. Muddiman, (2006) Generation and detection of multiply-charged peptides and proteins by matrix-assisted laser desorption electrospray ionization (MALDESI) Fourier transform ion cyclotron resonance

mass spectrometry, ***Journal of the American Society for Mass Spectrometry***, **17(12)**: 1712-1716.
28. M. Nazari, D. C. Muddiman, (2016) Polarity switching mass spectrometry imaging of healthy and cancerous hen ovarian tissue sections by infrared matrix-assisted laser desorption electrospray ionization (IR-MALDESI), ***Analyst***, **141(2)**: 595-605.
29. M. T. Bokhart, J. Manni, K. P. Garrard, M. Ekelöf, M. Nazari, D. C. Muddiman, (2017) IR-MALDESI mass spectrometry imaging at 50 micron spatial resolution, ***Journal of the American Society for Mass Spectrometry***, **28(10)**: 2099-2107.
30. K. C. Schäfer, J. Dénes, K. Albrecht, T. Szaniszló, J. Balog, R. Skoumal, ... & Z. Takáts, (2009) *In vivo*, *in situ* tissue analysis using rapid evaporative ionization mass spectrometry, ***Angewandte Chemie International Edition***, **48(44)**: 8240-8242.
31. J. M. Wiseman, D. R. Ifa, Q. Song, R. G. Cooks, (2006) Tissue imaging at atmospheric pressure using desorption electrospray ionization (DESI) mass spectrometry, ***Angewandte Chemie International Edition***, **45(43)**: 7188-7192.
32. A. L. Dill, D. R. Ifa, N. E. Manicke, Z. Ouyang, R. G. Cooks, (2009) Mass spectrometric imaging of lipids using desorption electrospray ionization, ***Journal of Chromatography B***, **877(26)**: 2883-2889.
33. J. B. Fenn, M. Mann, C. K. Meng, S. F. Wong, C. M. Whitehouse, (1989) Electrospray ionization for mass spectrometry of large biomolecules, ***Science***, **246(4926)**: 64-71.
34. S. Banerjee, S. Mazumdar, (2012) Electrospray ionization mass spectrometry: A technique to access the information beyond the molecular weight of the analyte, ***International Journal of Analytical Chemistry***, **2012:** 282574.
35. M. Fleming, S. Ravula, S. F. Tatishchev, H. L. Wang, (2012) Colorectal carcinoma: Pathologic aspects, ***Journal of Gastrointestinal Oncology***, **3(3)**: 153-173.
36. K. A. Lipinski, L. J. Barber, M. N. Davies, M. Ashenden, A. Sottoriva, M. Gerlinger, (2016) Cancer evolution and the limits of predictability in precision cancer medicine, ***Trends in Cancer***, **2(1)**: 49-63.
37. T. Liu, F. Peng, J. Yu, Z. Tan, T. Rao, Y. Chen, ... & J. Peng, (2019) LC-MS-based lipid profile in colorectal cancer patients: TAGs are the main disturbed lipid markers of colorectal cancer progression, ***Analytical and Bioanalytical Chemistry***, **411:** 5079-5088.
38. Y. Shen, M. Sun, J. Zhu, M. Wei, H. Li, P. Zhao, ... & J. Zhang, (2021) Tissue metabolic profiling reveals major metabolic alteration in colorectal cancer, ***Molecular Omics***, **17(3)**: 464-471.
39. J. Yang, H. Wei, Y. Zhou, C. H. Szeto, C., Li, Y. Lin, ... & J. Yu, (2022) High-fat diet promotes colorectal tumorigenesis through modulating gut microbiota and metabolites, ***Gastroenterology***, **162(1)**: 135-149.e2.
40. F. Chen, X. Dai, C. C. Zhou, K. X. Li, Y. J. Zhang, X. Y. Lou, ... & W. Cui, (2022) Integrated analysis of the faecal metagenome and serum metabolome reveals the role of gut microbiome-associated metabolites in the detection of colorectal cancer and adenoma, ***Gut***, **71(7)**: 1315-1325.
41. M. Kaufmann, N. Iaboni, A. Jamzad, D. Hurlbut, K. Y. M. Ren, J. F. Rudan, ... & C. J. Nicol, (2023) Metabolically active zones involving fatty acid elongation delineated by DESI-MSI correlate with pathological and prognostic features of colorectal cancer, ***Metabolites***, **13(4)**: 508.
42. V. Wu, J. Tillner, E. Jones, J. S. McKenzie, D. Gurung, A. Mroz, ... & Z. Takats, (2022) High resolution ambient MS imaging of biological samples by desorption electro-flow focussing ionization, ***Analytical Chemistry***, **94(28)**: 10035-10044.
43. A. M. Ganán-Calvo, (2007) Electro-flow focusing: The high-conductivity low-viscosity limit, ***Physical Review Letters***, **98(13)**: 134503.
44. T. P. Forbes, T. M. Brewer, G. Gillen, (2013) Desorption electro-flow focusing ionization of explosives and narcotics for ambient pressure mass spectrometry, ***Analyst***, **138(19)**: 5665-5673.
45. T. P. Forbes, E. Sisco, (2014) Chemical imaging of artificial fingerprints by desorption electro-flow focusing ionization mass spectrometry, ***Analyst***, **139(12)**: 2982-2985.
46. E. Agmon, B. R. Stockwell, (2017) Lipid homeostasis and regulated cell death, ***Current Opinion in Chemical Biology***, **39:** 83-89.
47. R. Wang, B. Li, S. M. Lam, G. Shui, (2020) Integration of lipidomics and metabolomics for in-depth understanding of cellular mechanism and disease progression, ***Journal of Genetics and Genomics***, **47(2)**: 69-83.
48. L. Zhan, C. Liu, K. Qi, L. Wu, Y. Xiong, X. Zhang, ... & Y. Pan, (2023) Enhanced imaging of endogenous metabolites by negative ammonia assisted DESI/PI mass spectrometry, ***Talanta***, 252: 123864.
49. J. Balog, T. Szaniszlo, K. C. Schaefer, J. Denes, A. Lopata, L. Godorhazy, ... & Z. Takats, (2010) Identification of biological tissues by rapid evaporative ionization mass spectrometry, ***Analytical Chemistry***, **82(17)**: 7343-7350.
50. P. M. Vaysse, I. Demers, M. F. van den Hout, W. van de Worp, I. G. Anthony, L. W. Baijens, ... & B. Kremer, (2022) Evaluation of the sensitivity of metabolic profiling by rapid evaporative ionization mass spectrometry: Toward more radical oral cavity cancer resections, ***Analytical Chemistry***, **94(19)**: 6939-6947.
51. R. Aebersold, J. Agar, I. Amster, M. S. Baker, C. R. Bertozzi, E. S. Boja, C. E. Costello, B. F. Cravatt, C. Fenselau, B. A. Garcia, Y. Ge, J. Gunawardena, ... & B, (2018) Zhang. How many human proteoforms are there? ***Nature Chemical Biology,*** **14:** 206-214.
52. L. M. Smith, N. L. Kelleher, Consortium for Top Down Proteomics. (2013) Proteoform: A single term describing protein complexity, ***Nature Methods***, **10:** 186-187.
53. R. B. Parekh, C. Rohlff, (1997) Post-translational modification of proteins and the discovery of new medicine, ***Current Opinion in Biotechnology***, **8(6)**: 718-723.
54. R. Yin, K. E. Burnum-Johnson, X. Sun, S. K. Dey, J. Laskin, (2019) High spatial resolution imaging of biological tissues using nanospray desorption electrospray ionization mass spectrometry, ***Nature Protocols***, **14:** 3445–3470.
55. C. J. Perez, A. K. Bagga, S. S. Prova, M. Yousefi Taemeh, D. R. Ifa, (2019) Review and perspectives on the applications of mass spectrometry imaging under ambient conditions, ***Rapid Communications in Mass Spectrometry***, **33:** 27-53.
56. J. Hanrieder, A. G. Ewing, (2014) Spatial elucidation of spinal cord lipid- and metabolite-regulations in amyotrophic lateral sclerosis, ***Scientific Reports,*** **4:** 5266.
57. M. Yang, H. Hu, P. Su, P. M. Thomas, J. M. Camarillo, J. B. Greer, B. P. Early, R. T. Fellers, N. L. Kelleher, J. Laskin, (2022) Proteoform-selective imaging of tissues using mass spectrometry, ***Angewandte Chemi***e, **134(29)**: e202200721.
58. L. M. Smith, P. M. Thomas, M. R. Shortreed, L. V. Schaffer, R. T. Fellers, R. D. LeDuc, T. Tucholski, Y. Ge, J. N. Agar, L. C. Anderson, J. Chamot-Rooke, J. Gault, J. A. Loo, ... & N. L. Kelleher, (2019) A five-level classification system for proteoform identifications, ***Nature Methods***, **16:** 939-940.
59. B. Borroni, E. Premi, A. Formenti, R. Turrone, A. Alberici, E.

Cottini, C. Rizzetti, P. Gasparotti, A. Padovani, (2015) Structural and functional imaging study in dementia with lewy bodies and Parkinson's disease dementia, ***Parkinsonism and Related Disorders***, **21:** 1049-1055.
60. F. Chollet, P. Payoux, (2022) Functional imaging for neurodegenerative diseases, ***La Presse Médicale***, **51:** 104121.
61. L. Gaetani, F. Paolini Paoletti, G. Bellomo, A. Mancini, S. Simoni, M. Di Filippo, L. Parnetti, (2020) CSF and blood biomarkers in neuroinflammatory and neurodegenerative diseases: Implications for treatment, ***Trends in Pharmacological Sciences***, **41:** 1023-1037.
62. R. Mejzini, L. L. Flynn, I. L. Pitout, S. Fletcher, S. D. Wilton, P. A. Akkari, (2019) ALS genetics; mechanisms, and therapeutics: Where are we now? ***Frontiers in Neuroscience***, **13:** 1310.
63. M. Kori, B. Aydın, S. Unal, K. Y. Arga, D. Kazan, (2016) Metabolic biomarkers and neurodegeneration: A pathway enrichment analysis of Alzheimer's disease, Parkinson's disease, and amyotrophic lateral sclerosis, ***OMICS***, **20(11)**: 645-661.
64. N. Bakkar, A. Boehringer, R. Bowser, (2015) Use of biomarkers in ALS drug development and clinical trials, ***Brain Research***, **1607:** 94-107.
65. A. Schmacher-Schuh, A. Bieger, W. V. Borelli, M. K. Portley, P. S. Awad, S. Bandres-Ciga, (2022) Advances in proteomic and metabolomic profiling of neurodegenerative diseases, ***Frontiers in Neurology,*** **12:** 792227.
66. J. S. Katzeff, F. Bright, K. Phan, J. J. Kril, L. M. Ittner, M. Kassiou, J. R. Hodges, O. Piguet, M. C. Kiernan, G. M. Halliday, W. S. Kim, (2022) Biomarker discovery and development for frontotemporal dementia and amyotrophic lateral sclerosis, ***Brain***, **145:** 1598-1609.
67. A. R. Buchberger, K. Delaney, J. Johnson, L. Li, (2017) Mass spectrometry imaging: A review of emerging advancements and future insights, ***Analytical Chemistry***, **90:** 240-265.
68. H. J. Jang, M. U. T. Le, J. H. Park, C. G. Chung, J. G. Shon, G. S. Lee, J. H. Moon, S. B. Lee, J. S. Choi, T. G. Lee, J. S. Choi, T. G. Lee, S. Yoon, (2021) Matrix-assisted laser desorption/ionization mass spectrometry imaging of phospholipid changes in a drosophila model of early amyotrophic lateral sclerosis, ***Journal of the American Society for Mass Spectrometry***, **32:** 2536-2545.
69. J. Hanrieder, P. Malmberg, A. G. Ewing, (2015) Spatial neuroproteomics using imaging mass spectrometry, *Biochimica et Biophysica Acta*, **1854(7)**: 718-731.
70. M. C. Bagley, K. P. Garrard, D. C. Muddiman, (2023) The development and application of matrix assisted laser desorption electrospray ionization: The teenage years, ***Mass Spectrometry Reviews***, **42(1):** 35-66.
71. M. T. Bokhart, D. C. Muddiman, (2016) Infrared matrix-assisted laser desorption electrospray ionization mass spectrometry imaging analysis of biospecimens, ***Analyst***, **141:** 5236.
72. R. B. Dixon, D. C. Muddiman, (2010) Study of the ionization mechanism in hybrid laser based desorption techniques, ***Analyst***, **135:** 880-882.
73. G. Robichaud, J. A. Barry, D. C. Muddiman, (2014) IR-MALDESI mass spectrometry imaging of biological tissue sections using ice as a matrix, ***Journal of the American Society for Mass Spectrometry***, **25:** 319-328.
74. A. Tu, D. C. Muddiman, (2019) Internal energy deposition in infrared matrix-assisted laser desorption electrospray ionization with and without the use of ice as a matrix, ***Journal of the American Society for Mass Spectrometry***, **30:** 2380-2391.
75. A. L. Sohn, L. Ping, J. D. Glass, N. T. Seyfried, E. C. Hector, D. Muddiman, (2022) Interrogating the metabolomic profile of amyotrophic lateral sclerosis in the post-mortem human brain by infrared matrix-assisted laser desorption electrospray ionization (IR-MALDESI) mass spectrometry imaging (MSI), ***Metabolites***, **12(11)**: 1096.
76. M. E. Umoh, E. B. Dammer, J. Dai, D. M. Duong, J. J. Lah, A. I. Levey, M. Gearing, J. D. Glass, N. T. Seyfried, (2018) A proteomic network approach across the ALS-FTD disease spectrum resolves clinical phenotypes and genetic vulnerability in human brain, ***EMBO Molecular Medicine***, **10:** 48-62.
77. A. Schousboe, S. Scafidi, L. K. Bak, H. S. Waagepetersen, M. C. McKenna, (2014) Glutamate metabolism in the brain focusing on astrocytes, ***Advances in Neurobiology***, **11:** 13-30.
78. X. X. Dong, Y. Wang, Z. H. Qin, (2009) Molecular mechanisms of excitotoxicity and their relevance to pathogenesis of neuro-degenerative diseases, ***Acta Pharmacologica Sinica***, **30:** 379-387.
79. G. D'Alessandro, E. Calcagno, S. Tartari, M. Rizzardini, R. W. Invernizzi, L. Cantoni, (2011) Glutamate and glutathione interplay in a motor neuronal model of amyotrophic lateral sclerosis reveals altered energy metabolism, ***Neurobiology of Disease***, **43:** 346-355.
80. D. Lanznaster, C. Bruno, J. Bourgeais, P. Emond, I. Zemmoura, A. Lefèvre, P. Reynier, S. Eymieux, E. Blanchard, P. Vourc'h, C. R. Andres, S. E. Bakkouche, O. Herault, L. Favard, P. Corcia, H. Blasco, (2022) Metabolic profile and pathological alterations in the muscle of patients with early-stage amyotrophic lateral sclerosis, ***Biomedicines***, 10: 1307.
81. J. J. Danon, T. A. Reekie, M. Kassiou, (2019) Challenges and opportunities in central nervous system drug discovery, ***Trends in Chemistry***, **1(6)**: 612-624.
82. V. K. Gribkoff, L. K. Kaczmarek, (2017) The need for new approaches in CNS drug discovery: Why drugs have failed, and what can be done to improve outcomes, ***Neuropharmacology***, **120:** 11-19.
83. L. Hutchinson, R. Kirk, (2011) High drug attrition rates--where are we going wrong? ***Nature Reviews Clinical Oncology***, **8(4)**: 189-190.
84. P. H. Hutson, J. A. Clark, A. J. Cross, (2017) CNS target identification and validation: avoiding the valley of death or naive optimism?, ***Annual Review of Pharmacology and Toxicology***, **57:** 171-187.
85. T. A. Ban, (2022). The role of serendipity in drug discovery, ***Dialogues in Clinical Neuroscience***, **8(3):** 335-44.
86. W. Zheng, N. Thorne, J. C. McKew, (2013) Phenotypic screens as a renewed approach for drug discovery, ***Drug Discovery Today***, **18(21-22)**: 1067-1073.
87. O. D. Howes, M. A. Mehta, (2021) Challenges in CNS drug development and the role of imaging, ***Psychopharmacology***, **238:** 1229-1230.
88. X. Pang, S. Gao, M. Ga, J. Zhang, Z. Luo, Y. Chen, ... & Z. Abliz, (2021) Mapping metabolic networks in the brain by ambient mass spectrometry imaging and metabolomics, ***Analytical Chemistry***, **93(17)**: 6746-6754.
89. J. He, C. Sun, T. Li, Z. Luo, L. Huang, X. Song, ... & Z. Abliz, (2018) A sensitive and wide coverage ambient mass spectrometry imaging method for functional metabolites based molecular histology, ***Advanced Science***, **5(11)**: 1800250.
90. M. Shariatgorji, A. Nilsson, E. Fridjonsdottir, T. Vallianatou, P.

Källback, L. Katan, ... & P. E. Andrén, (2019) Comprehensive mapping of neurotransmitter networks by MALDI–MS imaging, ***Nature Methods***, **16(10)**: 1021-1028.
91. E. Fridjonsdottir, R. Shariatgorji, A. Nilsson, T. Vallianatou, L. R. Odell, L. S. Schembri, ... & P. E. Andrén, (2021) Mass spectrometry imaging identifies abnormally elevated brain l-DOPA levels and extrastriatal monoaminergic dysregulation in l-DOPA-induced dyskinesia, ***Science Advances***, **7(2)**: eabe5948.
92. H. Kadar, G. Le Douaron, M. Amar, L. Ferrié, B. Figadere, D. Touboul, ... & R. Raisman-Vozari, (2014) MALDI mass spectrometry imaging of 1-methyl-4-phenylpyridinium (MPP+) in mouse brain, ***Neurotoxicity Research***, **25:** 135-145.
93. E. Sugiyama, M. M. Guerrini, K. Honda, Y. Hattori, M. Abe, P. Källback, ... & Y. Sugiura, (2019) Detection of a high-turnover serotonin circuit in the mouse brain using mass spectrometry imaging, ***iScience***, **20:** 359-372.
94. J. G. Swales, J. W. Tucker, M. J. Spreadborough, S. L. Iverson, M. R. Clench, P. J. Webborn, R. J. Goodwin, (2015) Mapping drug distribution in brain tissue using liquid extraction surface analysis mass spectrometry imaging, ***Analytical Chemistry***, **87(19)**: 10146-10152.
95. L. Huang, X. Mao, C. Sun, T. Li, X. Song, J. Li, ... & Z. Abliz, (2022) Molecular pathological diagnosis of thyroid tumors using spatially resolved metabolomics, ***Molecules***, **27(4)**: 1390.
96. P. Iruzubieta, M. T. Arias-Loste, L. Barbier-Torres, M. L. Martinez-Chantar, J. V. Crespo, (2015) The need for biomarkers in diagnosis and prognosis of drug-induced liver disease: Does metabolomics have any role? ***BioMed Research International***, **2015:** 386186.
97. L. L. Mazaleuskaya, K. Sangkuhl, C. F. Thorn, G. A. FitzGerald, R. B. Altman, T. E. Klein, (2015) PharmGKB summary: Pathways of acetaminophen metabolism at the therapeutic versus toxic doses, ***Pharmacogenetics and Genomics***, **25(8)**: 416-426.
98. M. R. McGill, H. Jaeschke, (2013) Metabolism and disposition of acetaminophen: recent advances in relation to hepatotoxicity and diagnosis, ***Pharmaceutical Research***, **30:** 2174-2187.
99. J. Y. Akakpo, M. W. Jaeschke, A. Ramachandran, S. C. Curry, B. H. Rumack, H. Jaeschke, (2021) Delayed administration of N-acetylcysteine blunts recovery after an acetaminophen overdose unlike 4-methylpyrazole, ***Archives of Toxicology***, **95:** 3377-3391.
100. J. Y. Akakpo, A. Ramachandran, L. Duan, M. A. Schaich, M. W. Jaeschke, B. D. Freudenthal, W. X. Ding, B. H. Rumack, H. Jaeschke, (2019) Delayed treatment with 4-methylpyrazole protects against acetaminophen hepatotoxicity in mice by inhibition of c-Jun N-terminal kinase, ***Toxicological Sciences***, **170(1)**: 57-68.
101. J. Y. Akakpo, A. Ramachandran, S. E. Kandel, H. M. Ni, S. C. Kumer, B. H. Rumack, H. Jaeschke, (2018) 4-Methylpyrazole protects against acetaminophen hepatotoxicity in mice and in primary human hepatocytes, ***Human and Experimental Toxicology***, **37(12)**: 1310-1322.
102. A. McEwen, C. Henson, (2015) Quantitative whole-body autoradiography: Past, present and future, ***Bioanalysis***, **7(5)**: 557-568.
103. E. G. Solon, (2012) Use of radioactive compounds and autoradiography to determine drug tissue distribution, ***Chemical Research in Toxicology***, **25(3)**: 543-555.
104. B. Prideaux, M. Stoeckli, (2012) Mass spectrometry imaging for drug distribution studies, ***Journal of Proteomics***, **75(16)**: 4999-5013.
105. O. Karlsson, J. Hanrieder, (2017) Imaging mass spectrometry in drug development and toxicology, ***Archives of Toxicology***, **91:** 2283-2294.
106. Y. N. Ho, L. J. Shu, Y. L. Yang, (2017) Imaging mass spectrometry for metabolites: Technical progress, multimodal imaging, and biological interactions, ***Wiley Interdisciplinary Reviews: Systems Biology and Medicine***, **9(5)**: e1387.
107. B. Balluff, L. A. McDonnell, (2018) Mass spectrometry imaging of metabolites, ***Clinical Metabolomics: Methods and Protocols***, **1730:** 345-357.
108. J. Y. Akakpo, M. W. Jaeschke, Y. Etemadi, A. Artigues, S. Toerber, H. Olivos, ... & A. Ramachandran, (2022) Desorption electrospray ionization mass spectrometry imaging allows spatial localization of changes in acetaminophen metabolism in the liver after intervention with 4-methylpyrazole, ***Journal of the American Society for Mass Spectrometry***, **33(11)**: 2094-2107.
109. H. J. Park, K. Friston, (2013) Structural and functional brain networks: From connections to cognition, ***Science***, **342(6158)**: 1238411.
110. R. Zhao, G. M. Pollack, (2009) Regional differences in capillary density, perfusion rate, and P-glycoprotein activity: A quantitative analysis of regional drug exposure in the brain, ***Biochemical Pharmacology***, **78(8)**: 1052-1059.
111. W. Z. Shou, (2020) Current status and future directions of high-throughput ADME screening in drug discovery, ***Journal of Pharmaceutical Analysis***, **10(3)**: 201-208.
112. H. H. Guo, C. L. Feng, W. X. Zhang, Z. G. Luo, H. J. Zhang, T. T. Zhang, ... & J. D. Jiang, (2019) Liver-target nanotechnology facilitates berberine to ameliorate cardio-metabolic diseases, ***Nature communications***, **10(1)**: 1981.
113. N. U. Khan, J. Ni, X. Ju, T. Miao, H. Chen, L. Han, (2021) Escape from abluminal LRP1-mediated clearance for boosted nanoparticle brain delivery and brain metastasis treatment, ***Acta Pharmaceutica Sinica B***, **11(5)**: 1341-1354.
114. L. Li, Q. Zang, X. Li, Y. Zhu, S. Wen, J. He, R. Zhang, Z. Abliz, (2023) Spatiotemporal pharmacometabolomics based on ambient mass spectrometry imaging to evaluate the metabolism and hepatotoxicity of amiodarone in HepG2 spheroids, ***Journal of Pharmaceutical Analysis***, **13:** 483-493.
115. E. Fahy, D. Cotter, M. Sud, S. Subramaniam, (2011) Lipid classification, structures and tools, ***Biochimica et Biophysica Acta***, **1811(11)**: 637-647.
116. F. Gibellini, T. K. Smith, (2010) The Kennedy pathway--de novo synthesis of phosphatidylethanolamine and phosphatidylcholine, ***IUBMB Life***, **62(6)**: 414-428.
117. W. Y. Sun, V. A. Tyurin, K. Mikulska-Ruminska, I. H. Shrivastava, T. S. Anthonymuthu, Y. J. Zhai, ... & V. E. Kagan, (2021) Phospholipase iPLA2β averts ferroptosis by eliminating a redox lipid death signal, ***Nature Chemical Biology***, **17(4)**: 465-476.
118. X. Luo, H. B. Gong, H. Y. Gao, Y. P. Wu, W. Y. Sun, Z. Q. Li, ... & R. R. He, (2021) Oxygenated phosphatidylethanolamine navigates phagocytosis of ferroptotic cells by interacting with TLR2, ***Cell Death and Differentiation***, **28(6)**: 1971-1989.
119. Y. Zhu, Q. Zang, Z. Luo, J. He, R. Zhang, Z. Abliz, (2022) An organ-specific metabolite annotation approach for ambient mass spectrometry imaging reveals spatial metabolic alterations of a whole mouse body, ***Analytical Chemistry***, **94(20)**: 7286-7294.
120. E. Fahy, S. Subramaniam, H. A. Brown, C. K. Glass, A. H. Merrill, R. C. Murphy, ... & E. A. Dennis, (2005) A comprehensive classification system for lipids1, ***Journal of Lipid Research***, **46(5)**: 839-861.

121. T. Harayama, H. Riezman, (2018) Understanding the diversity of membrane lipid composition, ***Nature Reviews Molecular Cell Biology***, **19(5)**: 281-296.
122. T. Cajka, O. Fiehn, (2016) Toward merging untargeted and targeted methods in mass spectrometry-based metabolomics and lipidomics, ***Analytical Chemistry***, **88(1)**: 524-545.
123. Y. H. Rustam, G. E. Reid, (2018) Analytical challenges and recent advances in mass spectrometry based lipidomics, ***Analytical Chemistry***, **90(1)**: 374-397.
124. X. Han, R. W. Gross, (2005) Shotgun lipidomics: Electrospray ionization mass spectrometric analysis and quantitation of cellular lipidomes directly from crude extracts of biological samples, ***Mass Spectrometry Reviews***, **24(3)**: 367-412.
125. J. L. Norris, R. M. Caprioli, (2013) Imaging mass spectrometry: A new tool for pathology in a molecular age, ***Proteomics-Clinical Applications***, **7(11-12)**: 733-738.
126. Y. Xiao, J. Deng, Y. Yao, L. Fang, Y. Yang, T. Luan, (2020) Recent advances of ambient mass spectrometry imaging for biological tissues: A review, ***Analytica Chimica Acta***, **1117:** 74-88.
127. C. Wu, A. L. Dill, L. S., Eberlin, R. G. Cooks, D. R. Ifa, (2013) Mass spectrometry imaging under ambient conditions, ***Mass Spectrometry Reviews***, **32(3)**: 218-243.
128. M. R. Weigand, M. Yang, H. Hu, C. Zensho, J. Laskin, (2022) Enhancement of lipid signals with ammonium fluoride in negative mode Nano-DESI mass spectrometry imaging, ***International Journal of Mass Spectrometry***, **478:** 116859.
129. A. Venter, P. E. Sojka, R. G. Cooks, (2006) Droplet dynamics and ionization mechanisms in desorption electrospray ionization mass spectrometry, ***Analytical Chemistry***, **78(24)**: 8549-8555.
130. D. I. Campbell, C. R. Ferreira, L. S. Eberlin, R. G. Cooks, (2012) Improved spatial resolution in the imaging of biological tissue using desorption electrospray ionization, ***Analytical and Bioanalytical Chemistry***, **404:** 389-398.
131. J. A. Stolee, B. Shrestha, G. Mengistu, A. Vertes, (2012) Observation of subcellular metabolite gradients in single cells by laser ablation electrospray ionization mass spectrometry, ***Angewandte Chemie International Edition***, **51(41)**: 10386-10389.
132. T. Wang, X. Cheng, H. Xu, Y. Meng, Z. Yin, X. Li, W. Hang, (2019) Perspective on advances in laser-based high-resolution mass spectrometry imaging, ***Analytical Chemistry***, **92(1)**: 543-553.
133. J. Wang, Z. Wang, F. Liu, L. Cai, J. B. Pan, Z. Li, ... & Y. Mo, (2018) Vacuum ultraviolet laser desorption/ionization mass spectrometry imaging of single cells with submicron craters, ***Analytical Chemistry***, **90(16)**: 10009-10015.
134. I. Kuznetsov, J. Filevich, F. Dong, M. Woolston, W. Chao, E. H. Anderson, ... & C. S. Menoni, (2015) Three-dimensional nanoscale molecular imaging by extreme ultraviolet laser ablation mass spectrometry, ***Nature Communications***, **6(1)**: 6944.
135. M. Niehaus, J. Soltwisch, M. E. Belov, K. Dreisewerd, (2019) Transmission-mode MALDI-2 mass spectrometry imaging of cells and tissues at subcellular resolution, ***Nature Methods***, **16(9)**: 925-931.
136. P. Nemes, A. A. Barton, Y. Li, A. Vertes, (2008) Ambient molecular imaging and depth profiling of live tissue by infrared laser ablation electrospray ionization mass spectrometry, ***Analytical Chemistry***, **80(12)**: 4575-4582.
137. A. Zavalin, E. M. Todd, P. D. Rawhouser, J. Yang, J. L. Norris, R. M. Caprioli, (2012) Direct imaging of single cells and tissue at sub-cellular spatial resolution using transmission geometry MALDI MS, ***Journal of Mass Spectrometry***, **47(11)**: 1473-1481.
138. Y. Meng, X. Song, R. N. Zare, (2022) Laser ablation electrospray ionization achieves 5 μm resolution using a microlensed fiber, ***Analytical Chemistry***, **94(28)**: 10278-10282.
139. M. van Faassen, R. Bischoff, K. Eijkelenkamp, W. H. de Jong, C. P. van der Ley, I. P. Kema, (2020) In matrix derivatization combined with LC-MS/MS results in ultrasensitive quantification of plasma free metanephrines and catecholamines, ***Analytical Chemistry***, **92(13)**: 9072-9078.
140. K. Murtada, F. de Andrés, A. Ríos, M. Zougagh, (2018) Determination of antidepressants in human urine extracted by magnetic multiwalled carbon nanotube poly (styrene-co-divinylbenzene) composites and separation by capillary electrophoresis, ***Electrophoresis***, **39(14)**: 1808-1815.
141. J. Bicker, A. Fortuna, G. Alves, A. Falcao, (2013) Liquid chromatographic methods for the quantification of catecholamines and their metabolites in several biological samples--a review, ***Analytica Chimica Acta***, **768:** 12-34.
142. D. G. Ferrer, A. G. García, J. Peris-Vicente, J. V. Gimeno-Adelantado, J. Esteve-Romero, (2015) Analysis of epinephrine, norepinephrine, and dopamine in urine samples of hospital patients by micellar liquid chromatography, ***Analytical and Bioanalytical Chemistry***, **407:** 9009-9018.
143. E. J. Anderson, J. T. Efird, A. C. Kiser, P. B. Crane, W. T. O'Neal, T. B. Ferguson, ... & A. P. Kypson, (2017) Plasma catecholamine levels on the morning of surgery predict post-operative atrial fibrillation, ***JACC: Clinical Electrophysiology***, **3(12)**: 1456-1465.
144. W. Atsumi, S. Tani, E. Tachibana, A. Hirayama, (2018) Combined evaluation of the plasma arginine vasopressin and noradrenaline levels may be a useful predictor of the prognosis of patients with acute decompensated heart failure, ***International Heart Journal***, **59(4)**: 791-801.
145. R. Belfort-DeAguiar, J. D. Gallezot, J. J. Hwang, A. Elshafie, C. W. Yeckel, O. Chan, ... & R. S. Sherwin, (2018) Noradrenergic activity in the human brain: A mechanism supporting the defense against hypoglycemia, ***The Journal of Clinical Endocrinology and Metabolism***, **103(6)**: 2244-2252.
146. D. S. Goldstein, G. Eisenhofer, J. J. Kopin, (2003) Sources and significance of plasma levels of catechols and their metabolites in humans, ***Journal of Pharmacology and Experimental Therapeutic***s, **305(3)**: 800-811.
147. W. Luo, T. A. van Beek, B. Chen, H. Zuilhof, G. I. Salentijn, (2022) Boronate affinity paper spray mass spectrometry for determination of elevated levels of catecholamines in urine, ***Analytica Chimica Acta***, **1235:** 340508.